

Ordinary and radiative muon capture on the proton and the pseudoscalar form factor of the nucleon

Véronique Bernard^{a*}, Thomas R. Hemmert^{b†}, Ulf-G. Meißner^{b‡}

^a Université Louis Pasteur, Laboratoire de Physique Théorique, F-67084 Strasbourg, France

^b Forschungszentrum Jülich, Institut für Kernphysik (Th), D-52425 Jülich, Germany

We calculate ordinary and radiative muon capture on the proton in an effective field theory of pions, nucleons and delta isobars. We work to second order in the small scale expansion. To this order, ordinary muon capture is not affected by the delta. We demonstrate that the isobar effects on the photon spectrum and total rate in radiative muon capture are of the order of a few percent, consistent with earlier findings in a more phenomenological approach. We also discuss the induced pseudoscalar form factor of the nucleon and comment on the existing discrepancy between the TRIUMF data and the theoretical calculations.

PACS: 23.40.-s,12.39.Fe,13.60-r

Keywords: Ordinary and radiative muon capture, pseudoscalar form factor, chiral effective field theory

*email: bernard@lpt6.u-strasbg.fr

†email: th.hemmert@fz-juelich.de

‡email: Ulf-G.Meissner@fz-juelich.de

I. INTRODUCTION

Ordinary and radiative muon capture on the proton at rest can be considered as an excellent testing ground for our understanding of dynamical and explicit chiral symmetry breaking in QCD. This stems from the fact that the typical momentum transfer in these reactions is very small, of the order of the muon mass, and one therefore can apply effective field theory methods, in particular baryon chiral perturbation theory. Ordinary muon capture (OMC),

$$\mu^-(l) + p(r) \rightarrow \nu_\mu(l') + n(r') , \quad (1.1)$$

where we have indicated the four-momenta of the various particles, allows to measure the so-called induced pseudoscalar coupling constant, g_P . This coupling constant is nothing but the value of the induced pseudoscalar form factor $G_P(t)$ at the four-momentum transfer for muon capture by the proton at rest, $g_P = m_\mu G_P(t = -0.88m_\mu^2/2M_N)$, with m_μ (M_N) the muon (nucleon) mass. Theoretically, it is dominated by the pion pole as given by the time-honored PCAC prediction, $g_P^{\text{PCAC}} = 8.89$. Adler and Dothan [1] as well as Wolfenstein [2] calculated the first correction to the PCAC result utilizing by now outdated (and in some cases misleading) methods. The ADW relation was derived directly from QCD Ward identities within the framework of heavy baryon chiral perturbation theory [3] and shown not to be affected by $\Delta(1232)$ effects in [4], $g_P^{\text{CHPT}} = 8.44 \pm 0.23$ (a similar calculation with a slightly different result was given in [5]). The presently available data have, however, too large error bars to discriminate between the pion pole prediction and its corrected version [6]. Furthermore, $G_P(t)$ for low four-momentum transfer squared can be extracted from charged pion electroproduction measurements [7]. The resulting momentum dependence of the induced pseudoscalar form factor is in agreement with the pion pole prediction. However, as in the case of the pseudoscalar coupling, the data are not precise enough to be sensitive to the small corrections found in [1] [2] [3].

While the momentum transfer in OMC is fixed, radiative muon capture (RMC),

$$\mu^-(l) + p(r) \rightarrow \nu_\mu(l') + n(r') + \gamma(k) , \quad (1.2)$$

has a variable t and one can get up to $t = m_\mu^2$ at the maximum photon energy of about $k \sim 100$ MeV, which is very close to the pion pole. This amounts approximately to a four times larger sensitivity to g_P in RMC than OMC. However, this increased sensitivity is upset by the very small partial branching ratio in hydrogen ($\sim 10^{-8}$ for photons with $k > 60$ MeV) and one thus has to deal with large backgrounds. Precisely for this reason only very recently a first measurement of RMC on the proton has been published [8]. The resulting number for g_P , which was obtained using a relativistic tree model including the Δ -isobar [9], came out significantly larger than expected from OMC, $g_P^{\text{RMC}} = 12.35 \pm 0.88 \pm 0.38 = 1.46 g_P^{\text{CHPT}}$. It should be noted that in this analysis the momentum dependence is entirely given in terms of the pion pole and the induced pseudoscalar coupling is obtained as a multiplicative factor from direct comparison to the photon spectrum and the partial RMC branching ratio (photon energies larger than 60 MeV). It was also argued in [8] that the atomic and molecular physics related to the binding of the muon in singlet and triplet atomic μp and ortho and para $p\mu p$ molecular states is sufficiently well under control.

The TRIUMF result spurred a lot of theoretical activity. While radiative muon capture had already been calculated in phenomenological tree level models a long time ago, see e.g. [10] [11] [12] [13] [9], heavy baryon chiral perturbation theory was also used at tree level including dimension two operators [14] and to one loop order [15]. The resulting photon spectra are not very different from the ones obtained in the phenomenological models, the most striking feature being the smallness of the chiral loops [15] hinting towards a good convergence of the chiral expansion. At present, the puzzling result from the TRIUMF experiment remains unexplained. It is, however, a viable possibility that the discrepancy does not come from the strong interactions but rather is related to the distribution of the various spin states of the muonic atoms. It is therefore mandatory to sharpen the theoretical predictions for the strong as well as the non-strong physics entering the experimental analysis.¹ Here, we wish to reanalyze RMC in the framework of the so-called small scale expansion [18,19], which allows to systematically include the Δ resonance into the effective field theory. Some preliminary results were reported in ref. [20]. One reason is to check the statement that the contribution from diagrams involving the Δ does not exceed 8% in the photon spectrum for photon energies above 60 MeV [13] and to perform this calculation in a systematic framework. In particular, we will consider the leading Δ effects which are of the order ϵ^2 in small scale expansion (where ϵ denotes a genuine small parameter, the pion mass, external momentum or the $N\Delta$ mass splitting). This extends in natural way the OMC study given in [4]. We remark that the pertinent expansion parameter m_μ/M_N is very small and one thus expects a quickly converging chiral

¹A recently proposed solution to the problem [16] based on a novel term has been shown to be inconsistent with gauge invariance in ref. [17]. The corrected term, which only gives a small contribution, is already contained in the work of ref. [15].

expansion. In the presence of the delta, however, naive dimensional analysis suggests corrections of the order of 30% due to the small nucleon–delta mass splitting, $m_\mu/(M_\Delta - M_N) \sim 3m_\mu/M_N$. In the small scale expansion, these effects already appear at second order and can therefore be analyzed in a tree level approach as presented here. Such an estimate appears to be in sharp contrast to the small effects found in the existing Feynman graph calculations. Clearly, these explicit Δ effects are not present in the calculation of [14] and are only indirectly contained via counterterms in the one loop result [15]. As we will show, the small scale expansion allows for a very transparent separation of the resonance and chiral pion effects.

The manuscript is organized as follows. In section 2, we briefly review how the Standard Model at low energies is mapped onto a chiral effective field theory. The ingredients of this field theory, which uses pions, nucleons and the delta isobar as degrees of freedom, are discussed in section 3. Section 4 is concerned with ordinary and radiative muon capture on the proton to second order in the small scale expansion. The status of the induced pseudoscalar form factor is reviewed and the analysis of the TRIUMF RMC experiment is critically assessed in section 5. Section 6 contains the summary and conclusions. Some more technical aspects of this work are relegated to the appendix.

II. FROM THE STANDARD MODEL TO THE EFFECTIVE FIELD THEORY

In this section we briefly summarize how QCD coupled to the standard electroweak theory is mapped onto the pertinent effective field theory. For that, we start with the electroweak Lagrangian. For our purpose, we only need the coupling of the charged currents to the charged massive gauge bosons (W_μ^\pm) and the coupling of the massless photon (A_μ) to the electromagnetic (em) current,

$$\mathcal{L}_{\text{int}}^{\text{SM}} = -\frac{g_2}{\sqrt{8}} \left\{ W_\mu^+(x) J_{\text{ch}}^\mu + W_\mu^-(x) J_{\text{ch}}^{\mu\dagger} \right\} - g_1 \cos \theta_W A_\mu(x) J_{\text{em}}^\mu + \mathcal{L}_{\text{ntl-wk}} \quad (2.1)$$

where the last term refers to the non-leptonic weak interactions. g_1 and g_2 are to the gauge couplings of the $U(1)_Y$ and the $SU(2)_L$ gauge groups and θ_W is the weak mixing (Weinberg) angle. In terms of the light quark and lepton fields the em and charged weak currents read

$$J_{\text{em}}^\mu = \frac{2}{3} \bar{u} \gamma^\mu u - \frac{1}{3} \bar{d} \gamma^\mu d - \bar{\mu} \gamma^\mu \mu + \dots \quad (2.2)$$

$$J_{\text{ch}}^\mu = \bar{u} \gamma^\mu (1 - \gamma_5) d + \bar{\nu}_\mu \gamma^\mu (1 - \gamma_5) \mu + \dots, \quad (2.3)$$

where the ellipsis refers to the terms we do not need in what follows. For constructing the effective field theory, it is most convenient to consider the QCD Lagrangian coupled to these gauge fields treated as external local sources, which transform locally under chiral symmetry [21]. With $e = g_1 \cos \theta_W$ and $W_\mu^- = \mathcal{V}_\mu^-(x) - \mathcal{A}_\mu^-(x)$, QCD coupled to these external sources takes the form

$$\begin{aligned} \mathcal{L}_{\text{QCD}}^{\text{ext,fields}} = & \mathcal{L}_{\text{QCD}}^0 + \bar{q} [\not{v}(x) - \not{a}(x) \gamma_5] q - \bar{q} [\not{s}(x) - i \not{p}(x)] q \\ & + \bar{q} [\not{v}^{(0)}(x) - \not{a}^{(0)}(x) \gamma_5] q - \bar{q} [\not{s}^{(0)}(x) - i \not{p}^{(0)}(x)] q, \end{aligned} \quad (2.4)$$

with q the bi-spinor of the light quark fields. For the case of RMC we are confronted with the following scenario of external sources²:

$$\not{s}(x) = 0, \quad (2.5)$$

$$\not{s}^{(0)}(x) = \hat{m} I, \quad (2.6)$$

$$\not{p}(x) = \not{p}^{(0)}(x) = 0, \quad (2.7)$$

$$\not{v}_\mu(x) = -e \frac{1}{2} \tau^3 A_\mu(x) - \left[\frac{g_2 V_{ud}}{\sqrt{8}} \left(\frac{1}{2} \tau^1 - \frac{i}{2} \tau^2 \right) \mathcal{V}_\mu^-(x) + \text{h.c.} \right], \quad (2.8)$$

$$\not{v}_\mu^{(0)}(x) = -e \frac{1}{6} I A_\mu(x), \quad (2.9)$$

$$\not{a}_\mu(x) = -\frac{g_2 V_{ud}}{\sqrt{8}} \left(\frac{1}{2} \tau^1 - \frac{i}{2} \tau^2 \right) \mathcal{A}_\mu^-(x) + \text{h.c.}, \quad (2.10)$$

$$\not{a}_\mu^{(0)} = 0, \quad (2.11)$$

²We are working in the limit of no isospin breaking, i.e. equal quark masses $m_u = m_d$ and no internal (virtual) photon effects.

with $s(x), p(x), v_\mu(x)$ and $a_\mu(x)$ scalar, pseudoscalar, vector and axial-vector fields, in order, in an obvious isospin (singlet and triplet) notation. V_{ud} is the pertinent element of the CKM matrix. Note that the term $\mathcal{L}_{\text{QCD}}^0$ in Eq.(2.4) is chirally symmetric. The explicit chiral symmetry breaking due to the current quark masses resides in the zeroth component of the external scalar source.

Having specified the external field environment we now analyze the required strong matrix elements for calculating OMC and RMC. First we define quark vector and axial-vector currents

$$V_\mu^a = \bar{q} \gamma_\mu T^a q, \quad (2.12)$$

$$A_\mu^a = \bar{q} \gamma_\mu \gamma_5 T^a q. \quad (2.13)$$

Here, the $T^a = \tau^a/2$ are the generators of $SU(2)$. With these definitions one then specifies the strong matrix elements which have to be calculated in the effective theory

$$a) \langle N | V_\mu^a | N \rangle, \quad (2.14)$$

$$b) \langle N | A_\mu^a | N \rangle, \quad (2.15)$$

$$c) \langle N | \mathcal{T} V_\mu^a V_\nu^b | N \rangle, \quad (2.16)$$

$$d) \langle N | \mathcal{T} V_\mu^a A_\nu^b | N \rangle, \quad (2.17)$$

with all possible combinations of the external fields of Eqs.(2.5-2.11) and \mathcal{T} denotes the conventional time-ordering operator. To proceed, we now have to specify the effective Lagrangian which will be used to calculate these matrix elements.

III. CHIRAL LAGRANGIANS

In this section, we briefly review the chiral Lagrangian underlying our calculation. While the meson part is standard, with the external momenta and the pion (light quark) mass counted as small parameters, for the meson–baryon system we include the nucleons as well as the $\Delta(1232)$ resonance. To systematically account for the effects of the latter, the $N\Delta$ mass splitting is considered as an additional small parameter. This is rooted in phenomenology and the large N_c limit of QCD, but not in the strict chiral limit, where the Δ decouples. These three small parameters are collectively denoted by ϵ .

A. Meson chiral perturbation theory

At low energies the chiral symmetry of QCD is spontaneously broken to the vectorial subgroup $SU(2)_V$: $SU(2)_L \times SU(2)_R \rightarrow SU(2)_V$. The strictures of the spontaneous and the explicit chiral symmetry breaking can be explored in terms of an effective field theory, chiral perturbation theory (CHPT). As a tool, one works with an effective Lagrangian, which consists of a string of terms with increasing dimension. For our purpose, we only need the first term in this expansion, the non-linear σ -model chirally coupled to the external sources,

$$\mathcal{L}_{\pi\pi}^{(2)} = \frac{F_0^2}{4} \text{Tr} [\nabla_\mu U^\dagger \nabla^\mu U + \chi^\dagger U + \chi U^\dagger] \quad (3.1)$$

with

$$U(x) = \exp \left\{ \frac{i}{F_0} \tau \cdot \pi(x) \right\}, \quad (3.2)$$

$$\nabla_\mu U = \partial_\mu U - i(\mathbf{v}_\mu + \mathbf{a}_\mu)U + iU(\mathbf{v}_\mu - \mathbf{a}_\mu), \quad (3.3)$$

$$\chi = 2B_0 \left(\mathbf{s} + s^{(0)} + i\mathbf{p} + i p^{(0)} \right). \quad (3.4)$$

The pions, which are nothing but integration variables, are collected in the matrix-valued field $U(x)$ and the explicit symmetry breaking due to the light quark masses is hidden in χ via the zeroth component of the scalar source. F_0 is the (weak) pion decay constant (in the chiral limit) and B_0 is related to the scalar quark condensate. We work in the standard scenario with $B_0 \gg F_0$. This specifies completely the meson part of the effective Lagrangian.

B. Including baryons: The small scale expansion

The nucleon–delta–pion system chirally coupled to the external fields can also be represented by a Lagrangian, which decomposes into a string of terms with increasing dimension. We work here in the heavy mass formulation, in which the nucleon and the delta are essentially considered as heavy, static sources. This allows to shuffle the baryon mass (M_B) dependence into a string of $1/M_B$ suppressed vertices and gives rise to a consistent power counting [22] [23] [19]. Denoting by N the (heavy) nucleon isodoublet field and by T_μ^i the Rarita–Schwinger representation of the heavy spin-3/2 field, the lowest order terms read

$$\begin{aligned}\mathcal{L}_{\pi N}^{(1)} &= \bar{N} [i v \cdot D + \dot{g}_A S \cdot u] N, \\ \mathcal{L}_{\pi \Delta}^{(1)} &= -\bar{T}_i^\mu [i v \cdot D^{ij} - \delta^{ij} \Delta_0 + \dots] g_{\mu\nu} T_j^\nu, \\ \mathcal{L}_{\pi N \Delta}^{(1)} &= \dot{g}_{\pi N \Delta} \left\{ \bar{T}_i^\mu g_{\mu\alpha} w_i^\alpha N + \bar{N} w_i^{\alpha\dagger} g_{\alpha\mu} T_i^\mu \right\},\end{aligned}\quad (3.5)$$

with $\Delta_0 = M_\Delta - M_0$ (M_0) being the nucleon–delta mass splitting (nucleon mass) in the chiral limit (to the order we are working, we can set $\Delta_0 = \Delta$). All other quantities Q in the chiral limit are denoted as \dot{Q} . Furthermore, v_μ and S_μ are the four–velocity and the spin–vector of the heavy nucleon. The various chiral covariant derivatives, chiral connections and vielbeins are (for details, we refer to [24] and [19])

$$\begin{aligned}D_\mu N &= (\partial_\mu + \Gamma_\mu - iv_\mu^{(s)})N, \\ v_\mu^{(s)} &= 3v_\mu^{(0)}, \\ \Gamma_\mu &= \frac{1}{2}[u^\dagger, \partial_\mu u] - \frac{i}{2}u^\dagger(\mathbf{v}_\mu + \mathbf{a}_\mu)u - \frac{i}{2}u(\mathbf{v}_\mu - \mathbf{a}_\mu)u^\dagger \equiv \tau^i \Gamma_\mu^i, \\ u_\mu &= iu^\dagger \nabla_\mu U u^\dagger \equiv \tau^i w_\mu^i, \\ D_\mu^{ij} T_\nu^j &= (\partial_\mu \delta^{ij} + C_\mu^{ij}) T_\nu^j, \\ C_\mu^{ij} &= \delta^{ij} \left(\Gamma_\mu - iv_\mu^{(s)} \right) - 2i\epsilon^{ijk} \Gamma_\mu^k,\end{aligned}\quad (3.6)$$

where i, j, k are isospin indices. At second order in the small scale expansion, we need the following terms

$$\begin{aligned}\mathcal{L}_{\pi N}^{(2)} &= \frac{1}{2M_0} \bar{N} \left\{ (v \cdot D)^2 - D^2 - ig_A (S \cdot D v \cdot u + v \cdot u S \cdot D) \right. \\ &\quad \left. - \frac{i}{2} [S^\mu, S^\nu]_- \left[(1 + \kappa_v) f_{\mu\nu}^+ + 2(1 + \kappa_s) v_{\mu\nu}^{(s)} \right] + \dots \right\} N,\end{aligned}\quad (3.7)$$

$$\mathcal{L}_{\pi N \Delta}^{(2)} = \bar{T}_i^\mu \frac{1}{2M_0} [b_1 i f_{+\mu\nu}^i S^\nu + \dots] N + \text{h.c.}\quad (3.8)$$

with

$$\begin{aligned}f_{\mu\nu}^\pm &= u^\dagger F_{\mu\nu}^R u \pm u F_{\mu\nu}^L u^\dagger \equiv \tau^i f_{\pm\mu\nu}^i, \\ F_{\mu\nu}^X &= \partial_\mu F_\nu^X - \partial_\nu F_\mu^X - i [F_\mu^X, F_\nu^X]; \quad X = L, R, \\ F_\mu^R &= \mathbf{v}_\mu + \mathbf{a}_\mu, \quad F_\mu^L = \mathbf{v}_\mu - \mathbf{a}_\mu, \\ v_{\mu\nu}^{(s)} &= \partial_\mu v_\nu^{(s)} - \partial_\nu v_\mu^{(s)}.\end{aligned}\quad (3.9)$$

Note that in $\mathcal{L}_{\pi N}^{(2)}$ only two low–energy constants (LECs) appear, which we have expressed in terms of the isoscalar and isovector anomalous magnetic moments, κ_s and κ_v , of the nucleon, respectively. The LEC b_1 is fixed from neutral pion photoproduction at threshold, $b_1 = 12.0$. We now have completely specified the effective Lagrangian needed to work out OMC and RMC to second order in the small scale expansion. The pertinent Feynman rules to perform these calculations are collected in appendix A.

IV. MUON CAPTURE

This section is concerned with the theoretical description of OMC and RMC. To keep the manuscript self–contained, we give all formulae necessary to calculate the capture rates.

A. Leptonic matrix elements

Consider first the purely leptonic part of the muon capture reaction. For OMC and RMC, we need the following two leptonic matrix elements:

$$\langle \nu_\mu | W_\mu^+ | \mu \rangle = -i \frac{g_2}{\sqrt{8}} \bar{\nu}_\mu(l') \gamma_\mu (1 - \gamma_5) \mu(l) , \quad (4.1)$$

$$\langle \nu_\mu \gamma | W_\mu^+ | \mu \rangle = -i \frac{g_2}{\sqrt{8}} \frac{e}{2l \cdot k} \bar{\nu}_\mu(l') \gamma_\mu (1 - \gamma_5) (2\epsilon^* \cdot l - k \cdot \epsilon^*) \mu(l) , \quad (4.2)$$

with ϵ_μ^* the polarization vector of the photon. The corresponding four-momenta have already been defined in Eq.(1.1) and Eq.(1.2), respectively.

B. Hadronic matrix elements

We now have to evaluate the strong matrix elements defined in Eqs.(2.14). Consider first the vector and axial correlators, cf. the first row in fig. 1, to second order in the small scale expansion,

$$\langle n | V_\mu^- | p \rangle^{(2)} = -i \frac{g_2 V_{ud}}{\sqrt{8}} \bar{n}(r') \left\{ v_\mu + \frac{1}{2M_N} (r + r')_\mu + \frac{1 + \kappa_v}{M_N} [S_\mu, S \cdot (r' - r)] \right\} p(r) , \quad (4.3)$$

$$\begin{aligned} \langle n | A_\mu^- | p \rangle^{(2)} = -i \frac{g_2 V_{ud}}{\sqrt{8}} \bar{n}(r') & \left\{ 2 g_A S_\mu - \frac{g_A}{M_N} S \cdot (r + r') v_\mu - 2 g_A R \frac{S \cdot (r' - r)}{(r' - r)^2 - m_\pi^2} (r' - r)_\mu \right. \\ & \left. + \frac{g_A}{M_N} R \frac{S \cdot (r + r') (v \cdot r' - v \cdot r)}{(r' - r)^2 - m_\pi^2} (r' - r)_\mu \right\} p(r) , \end{aligned} \quad (4.4)$$

where we have systematically shifted all appearing quantities to their physical values. Note that there is no isoscalar magnetic moment contribution in the vector correlator and the axial correlator includes, of course, the pion pole contribution. We turn to the vector–vector (VV) and vector–axial (VA) correlator. Working in the Coulomb gauge $\epsilon^* \cdot v = 0$ for the photon and making use of the transversality condition $\epsilon^* \cdot k = 0$, we find (the pertinent Feynman diagrams for the VV correlator are shown in the second row in fig. 1 and the ones for VA in figs. 2,3)

$$\begin{aligned} \langle n | \mathcal{T} V \cdot \epsilon^* V_\mu^- | p \rangle^{(2)} = -i \frac{g_2 V_{ud} e}{\sqrt{8}} \bar{n}(r') & \left\{ \frac{1 + \kappa_v}{M_N} [S_\mu, S \cdot \epsilon^*] - \frac{1}{2M_N} \epsilon_\mu^* \right. \\ & \left. + \frac{1}{M_N \omega} v_\mu [(1 + \kappa_v) [S \cdot \epsilon^*, S \cdot k] - \epsilon^* \cdot r] \right\} p(r) , \end{aligned} \quad (4.5)$$

$$\begin{aligned} \langle n | \mathcal{T} V \cdot \epsilon^* A_\mu^- | p \rangle^{(2)} = -i \frac{g_2 V_{ud} e}{\sqrt{8}} \bar{n}(r') & \times \\ & \left\{ 2 g_A \frac{S \cdot (r' - r)}{(r' - r)^2 - m_\pi^2} \times \left[\frac{2 \epsilon^* \cdot (l - l') (l - l')_\mu}{(l - l')^2 - m_\pi^2} - \epsilon_\mu^* \right] \right. \\ & - \frac{g_A}{M_N} \frac{(v \cdot r' - v \cdot r) S \cdot (r + r')}{(r' - r)^2 - m_\pi^2} \times \left[\frac{2 \epsilon^* \cdot (l - l') (l - l')_\mu}{(l - l')^2 - m_\pi^2} - \epsilon_\mu^* \right] \\ & - 2 g_A \left[1 + \frac{v \cdot l - v \cdot l'}{2M_N} \right] \frac{S \cdot \epsilon^* (l - l')_\mu}{(l - l')^2 - m_\pi^2} + \frac{g_A}{M_N} S \cdot \epsilon^* v_\mu \\ & + \frac{g_A}{M_N} \left[\frac{(2 + \kappa_s + \kappa_v) S^\alpha [S \cdot \epsilon^*, S \cdot k]}{\omega} + \frac{(\kappa_v - \kappa_s) [S \cdot \epsilon^*, S \cdot k] S^\alpha}{\omega} \right. \\ & \left. - \frac{2 S^\alpha \epsilon^* \cdot r}{\omega} \right] \times \left[g_{\mu\alpha} - R \frac{(l - l')_\alpha (l - l')_\mu}{(l - l')^2 - m_\pi^2} \right] \\ & + \frac{g_{\pi N \Delta} b_1}{3 M_N} \left[\frac{2 \Delta [k^\alpha S \cdot \epsilon^* - \omega v^\alpha S \cdot \epsilon^* - \epsilon^{*\alpha} S \cdot k]}{\Delta^2 - \omega^2} - \frac{4 S^\alpha [S \cdot \epsilon^*, S \cdot k]}{3 (\Delta + \omega)} \right. \\ & \left. + \frac{4 [S \cdot \epsilon^*, S \cdot k] S^\alpha}{3 (\Delta - \omega)} \right] \times \left[g_{\mu\alpha} - \frac{(l - l')_\alpha (l - l')_\mu}{(l - l')^2 - m_\pi^2} \right] \} p(r) , \end{aligned} \quad (4.6)$$

with $\omega = v \cdot k$ and $R = 1$ in QCD. We have introduced this factor multiplying the Born term contributions proportional to the induced pseudoscalar form factor for the later discussion. Note that the vector–vector correlator is free of delta effects to this order $\mathcal{O}(\epsilon^2)$, i.e. the delta only appears in the vector–axial correlator, cf. fig 3.

C. Ordinary Muon Capture

We work in the Fermi approximation of a static W_μ^- field, i.e. the gauge boson propagator is reduced to a point interaction (since the typical momenta involved are much smaller than the W mass),

$$\mathcal{M}_{\mu^- p \rightarrow \nu_\mu n} = \mathcal{M}^{\text{OMC}} = \langle \nu_\mu | W_\mu^+ | \mu \rangle i \frac{g^{\mu\nu}}{M_W^2} [\langle n | V_\nu^- | p \rangle - \langle n | A_\nu^- | p \rangle] . \quad (4.7)$$

Introducing the Fermi constant G_F via $G_F = g_2^2 \sqrt{2} / (8M_W^2)$, we define the square of the *spin-averaged* invariant matrix element to be

$$\frac{1}{4} \sum_{\sigma\sigma' ss'} |\mathcal{M}^{\text{OMC}}|^2 = \frac{G_F^2 V_{ud}^2}{2} L_{\mu\nu}^{(a)} H_{(a)}^{\mu\nu} . \quad (4.8)$$

With the normalizations

$$\begin{aligned} \sum_s \mu(l, s) \bar{\mu}(l, s) &= \frac{l + m_{\mu^-}}{2m_{\mu^-}}, \quad \sum_s \nu(l', s) \bar{\nu}(l', s) = l', \\ \sum_\sigma p_v(r, \sigma) \bar{p}_v(r, \sigma) &= P_v^+ \left(1 + \frac{v \cdot r}{2M_N} \right), \quad \sum_\sigma n_v(r', \sigma) \bar{n}_v(r', \sigma) = P_v^+ \left(1 + \frac{v \cdot r'}{2M_N} \right), \end{aligned} \quad (4.9)$$

one then obtains the symmetric tensors

$$L_{\mu\nu}^{(a)} = \frac{2}{m_{\mu^-}} \{ l_\mu l'_\nu - g_{\mu\nu} l \cdot l' + l'_\mu l_\nu + i \epsilon_{\mu\alpha\nu\beta} l^\alpha l'^\beta \} , \quad (4.10)$$

$$\begin{aligned} H_{\mu\nu}^{(a)} &= v_\mu v_\nu + g_A^2 (v_\mu v_\nu - g_{\mu\nu}) - g_A^2 \frac{\vec{r}'^2 + 2m_\pi^2}{(\vec{r}'^2 + m_\pi^2)^2} r'_\mu r'_\nu \\ &+ \frac{1 + g_A^2}{2M_N} (v_\mu r'_\nu + r'_\mu v_\nu) + \frac{g_A(1 + \kappa_v)}{M_N} i \epsilon_{\mu\nu}^{\alpha\beta} r'_\alpha v_\beta + \mathcal{O}(1/M_N^2) . \end{aligned} \quad (4.11)$$

Note that we have evaluated the tensors for the special kinematic condition of both the proton and the muon being at rest³, i.e. $l_\mu = (m_{\mu^-}, 0, 0, 0)$, $r_\mu = (0, 0, 0, 0)$. Furthermore, we have systematically truncated the hadronic tensor at $\mathcal{O}(1/M_N)$.

We now assume that the initial muon-proton system constitutes the ground-state of a bound system. We therefore replace the plane-wave wavefunction of the muon used so far in the calculation by the 1s Bohr-wavefunction $\Phi(x)_{1s}$ of a muonic atom. However, we note that our $\mathcal{O}(\epsilon^2)$ calculation is not sensitive to the extended structure of the proton – any dependence of the capture process on the electric/magnetic radius of the nucleon will only occur at $\mathcal{O}(\epsilon^3)$ [4]. For internal consistency we therefore have to assume that the capture on the “point-like” nucleon⁴ occurs at $x = 0$ and use

$$\Phi(0)_{1s} = \frac{\alpha^{3/2} \mu^{3/2}}{\sqrt{\pi}} , \quad (4.12)$$

with the reduced mass $\mu = M_N m_{\mu^-} / (M_N + m_{\mu^-})$ and $\alpha = e^2 / 4\pi\hbar c$ in the Heaviside-Lorentz convention. We can therefore calculate the spin-averaged rate of ordinary muon capture via

³This approximation is well-justified due to the low binding energy $E \approx 2.5$ keV of an s-wave muonic atom as compared to the muon mass.

⁴In a systematic $\mathcal{O}(\epsilon^3)$ analysis one has to calculate the overlap between the Bohr-wavefunction and the respective proton-neutron transition form factors.

$$\Gamma_{\text{OMC}} = |\Phi(0)_{1s}|^2 \int \frac{d^3 r'}{(2\pi)^3 J_n} \frac{d^3 l'}{(2\pi)^3 J_\nu} (2\pi)^4 \delta^4(r + l - r' - l') \frac{1}{4} \sum_{\sigma\sigma' ss'} |\mathcal{M}^{\text{OMC}}|^2 \quad (4.13)$$

with the normalization factors $J_\nu = 2E_\nu$, $J_n = 1 + v \cdot r'/M_N$. Systematically evaluating all expressions at $\mathcal{O}(\epsilon^2)$ accuracy one obtains

$$\begin{aligned} \Gamma_{\text{OMC}}^{(2)} &= \frac{\alpha^3 G_F^2 V_{ud}^2 m_{\mu^-}^5}{2\pi^2 (m_\pi^2 + m_{\mu^-}^2)^2} \left\{ (2g_A^2 + 1) m_{\mu^-}^4 + 2(2g_A^2 + 1) m_{\mu^-}^2 m_\pi^2 + (3g_A^2 + 1) m_\pi^4 \right. \\ &\quad + \frac{2 m_{\mu^-}}{(m_\pi^2 + m_{\mu^-}^2) M_N} \left[(g_A(1 + \kappa_v) - 5g_A^2 - 2) (m_{\mu^-}^6 + 3m_{\mu^-}^4 m_\pi^2) \right. \\ &\quad \left. \left. + (3g_A(1 + \kappa_v) - 16g_A^2 - 6) m_{\mu^-}^2 m_\pi^4 \right] \right\} + \mathcal{O}(1/M_N^2) \\ &= (247 - 59) \times \text{s}^{-1} + \mathcal{O}(1/M_N^2) \\ &= 188 \times \text{s}^{-1} \end{aligned} \quad (4.14)$$

Here we have used the coupling constants and masses as given in table I. Note that the $\mathcal{O}(\epsilon^2)$ contribution amounts to a correction of less than 25% of the leading term, indicating that muon capture on a proton really constitutes a system with a well behaved chiral expansion. We also note that in the case of no explicit chiral symmetry breaking (i.e. in the chiral limit $m_\pi = 0$) one would expect the spin-averaged capture rate to be

$$\begin{aligned} \Gamma_{\text{OMC}}^\chi &= (214 - 46) \times \text{s}^{-1} + \mathcal{O}(1/M_N^2) \\ &= 168 \times \text{s}^{-1}. \end{aligned} \quad (4.15)$$

The physical reason for the nice stability of perturbative calculations for OMC is of course the fact that contributions of order n are suppressed by $(m_i/\Lambda_\chi)^{n-1}$, with $i = \pi, \mu$ and $\Lambda_\chi \sim M_N \sim 1\text{GeV}$. Note that one can also retain the higher order *kinematical* corrections starting at order $1/M_N^2$. To be more precise, this refers to the energy-momentum relation between the various particles, the mass term appearing in the various projection operators and the phase space. In that case, only the various correlators (A,V,AV,VV) are truncated at order $1/M_N$. Using this approximation, the total rate is $\Gamma_{\text{OMC}} = 195 \text{s}^{-1}$, i.e. only 3% different from the one given in eq.(4.14). We remark already at this point that in the case of RMC, it is mandatory to retain these higher order terms if one stays at a low order in the small scale expansion as done here.

We now consider the general polarized case. The muon and the proton can form a singlet or a triplet atomic state. These various spin states are obtained by using the following projection operators for the muon,

$$\begin{aligned} \mu(l, 1/2)\bar{\mu}(l, 1/2) &= \frac{1}{2}(1 + \gamma_5 \not{s}) \frac{\not{l} + m_\mu}{2m_\mu}, \\ \mu(l, \pm 1/2)\bar{\mu}(l, \mp 1/2) &= \frac{\not{l} + m_\mu}{2m_\mu(E_\mu + m_\mu)} \gamma_5 \gamma_0 \frac{1}{2}(\gamma_1 \pm i\gamma_2) \gamma_0 (\not{l} + m_\mu), \end{aligned} \quad (4.16)$$

and similarly for the proton,

$$\begin{aligned} u(l, 1/2)\bar{u}(l, 1/2) &= \frac{1}{2}(1 + \gamma_5 \not{s}) \frac{1}{2}(1 + \not{v}) \left(1 + \frac{\not{v} \cdot \not{r}}{2M_N}\right), \\ u(l, \pm 1/2)\bar{u}(l, \mp 1/2) &= \frac{1}{2}(1 + \not{v}) \frac{\not{p} + m_\mu}{2M_N(E_N + M_N)} \gamma_5 \gamma_0 \frac{1}{2}(\gamma_1 \pm i\gamma_2) \gamma_0 (\not{p} + M_N) \frac{1}{2}(1 + \not{v}), \end{aligned} \quad (4.17)$$

using $(1 + \not{v})(\not{p} + M_N) = (1 + \not{v})(\not{p} + 2M_N)$. From the singlet (S) and triplet (T) atomic states, one can form the so-called para (P) and ortho (O) states by the following linear combinations,

$$\begin{aligned} P &= \frac{1}{4}(3T + S), \\ O &= \frac{1}{4}(T + 2S), \end{aligned} \quad (4.18)$$

where the singlet is the usual state $(1/\sqrt{2})(|\uparrow,\downarrow\rangle - |\downarrow,\uparrow\rangle)$ in terms of the muon and proton spins and the triplet accordingly. Note that the para state is often referred to as the statistical mixture. For the total capture rates of singlet and the triplet states, we find the following decomposition into leading and next-to-leading order pieces in the $1/M_N$ expansion,

$$\begin{aligned}\Gamma_{\text{sing}} &= (957.2 - 231.3 \text{ GeV}/M_N) \times \text{s}^{-1}, \\ \Gamma_{\text{trip}} &= (10.28 + 3.51 \text{ GeV}/M_N) \times \text{s}^{-1}.\end{aligned}\quad (4.19)$$

These results agree nicely with the ones of Primakoff [25], $\Gamma_{\text{sing}} = 636 \text{ s}^{-1}$ and $\Gamma_{\text{trip}} = 13 \text{ s}^{-1}$. As noted before, one does not have to truncate the kinematical $1/M_N$ corrections at this order. We find that while such terms are very small for the singlet case, the $1/M_N^2$ corrections for the (small) triplet are about one third of the ones of order $1/M_N$, while higher terms are again tiny.

D. Radiative muon capture

1. Total capture rates

In the static approximation for the W-boson, the pertinent matrix element for RMC decomposes into two terms,

$$\begin{aligned}\mathcal{M}_{\mu^- p \rightarrow \nu_\mu n \gamma} &= \langle \nu_\mu | W_\mu^+ | \mu \rangle i \frac{g^{\mu\nu}}{M_W^2} [\langle n | \mathcal{T} V \cdot \epsilon^* V_\nu^- | p \rangle - \langle n | \mathcal{T} V \cdot \epsilon^* A_\nu^- | p \rangle] \\ &\quad + \langle \nu_\mu | W_\mu^+ | \mu \rangle i \frac{g^{\mu\nu}}{M_W^2} [\langle n | V_\nu^- | p \rangle - \langle n | A_\nu^- | p \rangle],\end{aligned}\quad (4.20)$$

so that its square in the spin-averaged case can be written as a sum of four terms, with both photons coming either from the hadronic or the leptonic side and two mixed terms, i.e.

$$\frac{1}{4} \sum_{\sigma\sigma' ss' \lambda\lambda'} |\mathcal{M}^{RMC}|^2 = \frac{e^2 G_F^2 V_{ud}^2}{2} \left[L_{\mu\nu}^{(a)} H_{(d)}^{\mu\nu} + \left(\sum_{\lambda\lambda'} L_{\mu\nu}^{(b)} H_{(c)}^{\mu\nu} + L_{\mu\nu}^{(c)} H_{(b)}^{\mu\nu} \right) + L_{\mu\nu}^{(d)} H_{(a)}^{\mu\nu} \right], \quad (4.21)$$

with λ, λ' the photon helicities. Explicit expressions for the various tensors are not given here because they are lengthy and not illuminating. We also note that standard packages like REDUCE can not be used straightforwardly to obtain these tensors since the cyclicity of the trace in the presence of γ_5 matrices is not fulfilled. The total decay rate is given by:

$$\Gamma_{\text{tot}} = \frac{|\Phi(0)_{1s}|^2}{16\pi^4} \int_0^\pi \sin\theta d\theta \int_0^{\omega_{\text{max}}} d\omega \omega l'_0 \left(1 - \left(\frac{m_\mu - \omega(1 - \cos\theta)}{M_N} \right) \right) \frac{1}{4} \sum_{\sigma\sigma' ss' \lambda\lambda'} |\mathcal{M}^{RMC}|^2, \quad (4.22)$$

with $\omega = k_0$ the photon energy. The direction of the photon defines the z-direction and θ in eq.(4.22) is the polar angle of the outgoing lepton with respect to this direction. The maximal photon energy is given by

$$\omega_{\text{max}} = m_\mu \left(1 + \frac{m_\mu}{2M_N} \right) \left(1 + \frac{m_\mu}{M_N} \right)^{-1}. \quad (4.23)$$

Furthermore, the energy of the outgoing lepton follows from energy conservation,

$$l'_0 = m_N - \omega - \frac{m_\mu^2}{M_N} + \frac{\omega(1 - \cos\theta)(m_\mu - \omega)}{M_N} + \mathcal{O}(1/M_N^2). \quad (4.24)$$

The rates for the singlet and triplet states can be obtained by the projection formalism outlined in sec.IV C, we refrain from spelling out the corresponding formulae here. Note that we do not expand all kinematical factors in powers of $1/M_N$ since in case of the small singlet, the contribution from the terms starting at order $1/M_N^2$ can not be neglected.⁵ In fact, a strict truncation at $1/M_N$ (which we also performed) would lead to an unphysical negative

⁵Note the reversal of the relative size of the singlet to triplet contribution as compared to the case of OMC.

singlet capture rate. For the much bigger triplet, these higher order corrections are much less important. We remark that in ref. [14] no strict $1/M_N$ expansion was performed, only at some places these authors used the leading order results, e.g. for the nucleon energy by neglecting the recoil term. Only if one goes to a sufficiently high order in the small scale expansion, the truncation of these kinematical factors can be justified. In table II we have collected the results for the case without ($b_1 = 0$) and with the delta ($b_1 = 12$). Note that the delta contribution only amounts to a 1.5 percent change in the total capture rate (as explained below). The leading order terms, which scale as M_N^0 and are free of delta effects, lead to a total rate of $\Gamma_{\text{tot}} = 66 \times \text{s}^{-1}$, which agrees with the leading order result of ref. [14], $\Gamma_{\text{tot}} = 61 \times \text{s}^{-1}$. The small difference can be traced back to the different values of some of their input parameters. Our next-to-leading order corrections are somewhat larger than theirs but agree with the ones found in ref. [15].

2. Photon spectrum

The photon spectrum $d\Gamma/d\omega$ can be obtained straightforwardly from eq.(4.22). We refrain from giving the lengthy formulae for the various atomic states here. We have calculated the photon spectra for the case with and without the delta. The resulting curves are very similar, in fig.4 we show the case including the Δ for the standard couplings, $g_{\pi N \Delta} \times b_1 = 1.05 \times 12 = 12.6$ for the singlet, triplet, para and ortho states. The relative changes for all states due to the Δ are shown in fig.5. With the exception of the small singlet, the Δ effects amount to less than 5% for all photon energies. Only in the case of the singlet, a more pronounced influence of the Δ is observed. We note that these results are very similar to the ones found by Beder and Fearing [13,9] for the spectra and the relative contribution from the spin-3/2 resonance, although their calculation is based on a very different approach. Even the result for the singlet is comparable though not identical to the one of Beder and Fearing. It changes sign for photon energies of about 74 MeV. Like for the case of the small triplet in OMC, it is expected that the small singlet (for RMC) is more sensitive to $1/M_N$ corrections. We have also increased the coupling b_1 to values of 24 and 60 thus enhancing the Δ contribution by a factor of 2 and 5, respectively. We find very little sensitivity to this, e.g. the maximum in the photon spectrum for the para state changes from $1.47 \text{ GeV}^{-1} \text{s}^{-1}$ for $b_1 = 12$ to $1.55 \text{ GeV}^{-1} \text{s}^{-1}$ for $b_1 = 60$. Correspondingly, the total decay rate for the para state is increased by 7%. The smallness of the delta has two reasons. First, as noted before, it only appears at the first subleading order. Second, its sole contribution at that order is in axial-vector correlator, but not in the other three correlators. This already leads to a statistical suppression as compared to the nucleon terms. Third, despite the largeness of the coupling $g_{\pi N \Delta} \times b_1$ (remember that b_1 is related to the dominant $M1 N\Delta$ transition), the delta contribution to the VA-correlator is still smaller than the one from the nucleon, which is enhanced by the large isovector magnetic moment. The dominant axial and axial-vector contribution comes indeed from the leading pion pole, which is not affected by the Δ . To quantify these statements, let us for a moment consider the deltaless theory with $b_1 = 0$. If one switches off the complete contribution from the axial correlator, eq.(4.4), the singlet rate is enhanced by a factor of 1.7, whereas the triplet is decreased by a factor of about 170!. Consequently, we then have $\Gamma_{\text{tot}} \simeq 7 \times \text{s}^{-1}$, which is an order of magnitude smaller than the value given in Table II. If one sets $\kappa_s = \kappa_v = 0$ in the V, VV and AV correlators, the singlet rate increases by a factor of about 2.7 and the triplet rate decreases by a factor of 1.3, leading to a total rate of $68 \times \text{s}^{-1}$.

It is also instructive to consider the chiral limit, $m_\pi = 0$. To be specific, we discuss the deltaless theory⁶. To leading order in $1/M_N$, one encounters a pole at $\omega = m_\mu/2$ in the A and AV correlators. This can be seen by looking at pion pole terms in the chiral limit, which take the form

$$\frac{1}{(l - l')^2} = \frac{1}{m_\mu^2 - 2m_\mu l'_0} , \quad (4.25)$$

and using the leading order result $l'_0 = m_\mu - \omega + \mathcal{O}(1/M_N)$, cf. Eq.(4.24). This well-known Bethe-Heitler pole is independent of the angular variable x . The condition for this pole to appear is that the pion mass has to be below the muon mass. For zero pion mass, there is another pole at the same energy for $x = -1$ stemming from the terms $\sim (r - r')^{-1}$. Since this case is hypothetical, we do not want to further dwell on this topic. The chiral limit photon spectra of the next-to-leading order calculation are shown in Fig.6 for $b_1 = 0$. We remark that these spectra are very different from the ones with the physical pion mass due to the abovementioned singularities. We also point out that the pion mass effects are larger in RMC than in the OMC case discussed above. In particular, setting e.g. $m_\pi = 125 \text{ MeV}$, the rate in the para state (total rate) increases to $99 \times \text{s}^{-1}$. We will discuss the implications of the TRIUMF measurement in the following section.

⁶The results including the Δ are very similar.

V. THE PSEUDOSCALAR FORM FACTOR OF THE NUCLEON

A. Definitions and general remarks

The electroweak structure of a nucleon is typically encoded via 6 form factors (e.g. ref. [4]). Muon captures provides us with the opportunity to study the weak axial structure of a nucleon. In the absence of second class currents the corresponding relativistic matrix element of the hadronic axial current reads

$$\langle n|A_\alpha^-|p\rangle = \bar{n}(p_2) \left[G_A(q^2) \gamma_\alpha \gamma_5 + \frac{G_P(q^2)}{2M_N} q_\alpha \gamma_5 \right] p(p_1). \quad (5.1)$$

Here, $G_A(q^2)$ and $G_P(q^2)$ are the axial and the induced pseudoscalar form factor, respectively. While $G_A(q^2)$ can be extracted from (anti)neutrino–proton scattering or charged pion electroproduction data, $G_P(q^2)$ is harder to pin down and in fact *constitutes the least known nucleon form factor*. In Fig.7 we present the “world data” for $G_P(q^2)$. There are two curves shown in Fig.7 to display the difference between the usual pion-pole parameterization for $G_P(q^2)$ and analyses that take into account the full chiral structure of the form factor [3], yielding

$$G_P^\chi(q^2) = \frac{4M_N g_{\pi NN} F_\pi}{m_\pi^2 - q^2} - \frac{2}{3} g_A M_N^2 r_A^2. \quad (5.2)$$

In ref. [4] it was also shown that the leading nucleon resonance $\Delta(1232)$ does not modify this result. Note that the terms multiplied by the constant R in eqs.(4.4,4.6) are proportional to this form factor. In the kinematical region of RMC, which mainly lies to the “left” of the OMC point in Fig.7 the structure effect proportional to the axial radius r_A is expected to play only a small role. Certainly, the present experimental uncertainties both in OMC [6] and in RMC [8] are too large to distinguish between the two curves, but new efforts are under way [26]. Finally we want to emphasize that there exists another window on $G_P(q^2)$ —pion electroproduction. So far there has only been one experiment [7] that took up the challenge, with the results shown in Fig.7. In this kinematical regime the structure proportional to r_A produces the biggest effect and a new dedicated experiment should be able to identify it — thereby enhancing our knowledge of this poorly known form factor considerably! In fact, at the Mainz Microtron MAMI-B a dedicated experiment has been proposed to measure the axial and the induced pseudoscalar form factors by means of charged pion electroproduction at low momentum transfer [27].

B. Discussion of the TRIUMF result for g_P

The photon spectra discussed in section IV D 2 allow in principle to determine the induced pseudoscalar form factor. The TRIUMF result for g_P is obtained by multiplying the terms proportional to the pseudoscalar form factor with a constant denoted R (the momentum dependence assumed to be entirely given by the pion pole). The value of R is then extracted using the model of Fearing et al. to match the partial rate for photon energies larger than 60 MeV. If we perform such a procedure, we get a similar shift in the partial photon spectra (using the same weight factors for the various $\mu - p$ states as given in ref. [8]). It is, however, obvious from our analysis that such a procedure is not legitimate. By artificially enhancing the contribution $\sim g_P$ (to simulate this procedure, we have introduced the factor R in eqs.(4.4,4.6)), one mocks up a whole class of new contact and other terms not present in the Born term model. To demonstrate these points in a more quantitative fashion, we show in fig.8 the partial branching fraction for our calculation in comparison to the one with g_P enhanced by a factor 1.5 and a third curve, which is obtained by increasing g_P only by 15%, take $b_1 = 24$ (i.e. enhancing this coupling by a factor of two) and use $\Delta = 273$ MeV, since in the dispersion theoretical analysis of pion–nucleon scattering the pole in the P_{33} partial wave is located at $W = 1210$ MeV. This is shown in fig.8 by the dashed line and it shows that such a combination of small effects can explain most (but not all) of the shift in the spectrum. This is further sharpened by using now the neutral pion mass of 134.97 MeV instead of the charged pion mass, leading to the dotted curve in fig.8. Since the pion mass difference is almost entirely of electromagnetic origin, one might speculate that isospin–breaking effects should not be neglected (as done here and all other existing calculations). The situation is reminiscent of the sigma term analysis, where many small effects combine to give the sizeable difference between the sigma term at zero momentum transfer and at the Cheng-Dashen point. We further point out that although the present investigation combined with the findings in ref. [15] does not seem to give any large new term at order ϵ^2 or from the chiral loops at third order, it can not be excluded that one–loop graphs with insertions from the dimension two chiral Lagrangian (which are formally of fourth order) can give rise to larger corrections than the third order loop and tree terms calculated in ref. [15]. In fact, as we noted before, the photon spectrum is more sensitive to changes in the anomalous magnetic moments than

to the induced pseudoscalar coupling. Therefore it can be speculated that one-loop graphs with exactly one insertion $\sim \kappa_v$ can generate large corrections. This appears plausible but needs to be supported by a fourth order calculation. Such a mechanism would, however, be much more natural than the simple rescaling of g_P based on tree level diagrams only. It is well-known from e.g. neutral pion photoproduction that loop graphs can completely invalidate a Born graph calculation.

VI. SUMMARY

In this manuscript, we have considered ordinary and radiative muon capture on the proton in the framework of the small scale expansion to second order in small momenta, $\mathcal{O}(\epsilon^2)$. We have also discussed the induced pseudoscalar form factor of the nucleon and its determination from the TRIUMF RMC data. The pertinent results of this investigation can be summarized as follows:

- (i) To second order in the small scale expansion, ordinary muon capture is not affected by delta isobar effects. The next-to-leading order contribution for the total capture rate amounts to a 25% correction of the leading term. This is in agreement with naive dimensional counting, which lets one expect corrections of the size m_μ/Λ_χ . This calculation involves very few and well-controlled parameters.
- (ii) To the same order, we have considered radiative muon capture. The delta appears at first non-leading order, $1/M_N$, and its effects on the total capture rate and the photon spectrum are of the order of a few percent. The smallness of the delta contribution is due to a combination of effects as discussed in section IV D 2. This agrees with earlier findings in a more phenomenological approach [9]. Isobar effects can therefore not resolve the discrepancy between the TRIUMF measurement for the partial decay width $\Gamma(\omega > 60 \text{ MeV})$ and the theoretical predictions. We have, however, pointed out a severe loophole concerning the extraction of g_P as done in ref. [8]. In our opinion the most probable explanation of the discrepancy is a combination of many small effects.
- (iii) The induced pseudoscalar form factor measured in charged pion electroproduction is not very well determined, but clearly is in agreement with the one-loop chiral perturbation theory prediction [3]. A more precise measurement for small invariant momentum transfer squared is called for [27].

APPENDIX A: FEYNMAN RULES

In this appendix, we collect the pertinent Feynman rules for calculating OMC and RMC. These read:

Isovector vector source in (q_μ) , nucleon:

$$i v \cdot \mathbf{v} + \frac{i}{2M_0} ((r_i + r_f) \cdot \mathbf{v} - (r_i + r_f) \cdot v v \cdot \mathbf{v}) + \frac{i}{M_0} (1 + \kappa_v) [S \cdot \mathbf{v}, S \cdot q] , \quad (\text{A.1})$$

Isovector axial source in, nucleon:

$$i 2 \dot{g}_A S \cdot \mathbf{a} - i \frac{\dot{g}_A}{M_0} S \cdot (r_i + r_f) v \cdot \mathbf{a} , \quad (\text{A.2})$$

Isovector axial source in, pion out (k_μ) :

$$F_0 \frac{1}{2} \text{Tr}[\tau^i \mathbf{a}^\dagger \cdot k + \mathbf{a} \cdot k \tau^i] , \quad (\text{A.3})$$

Isovector axial source, vector source, pion:

$$- \frac{F_0}{2} \text{Tr}\{[\mathbf{v}_\mu, \tau^i] \mathbf{a}^\mu + \mathbf{a}_\mu [\mathbf{v}^\mu, \tau^i]\} , \quad (\text{A.4})$$

2 vector sources in, nucleon:

$$\frac{i}{2M_0} \left\{ (\mathbf{v} + v^{(s)})^2 - \left[v \cdot (\mathbf{v} + v^{(s)}) \right]^2 - (1 + \kappa_v) [S^\mu, S^\nu] [\mathbf{v}_\mu, \mathbf{v}_\nu] \right\} , \quad (\text{A.5})$$

vector source and isovector axial source in, nucleon:

$$-i \frac{\dot{g}_A}{M_0} \left[S \cdot \left(\mathbf{v} + v^{(s)} \right) v \cdot \mathbf{a} + v \cdot \mathbf{a} S \cdot \left(\mathbf{v} + v^{(s)} \right) \right] , \quad (\text{A.6})$$

Δ_μ^i in, nucleon and vector source (k_μ) out:

$$+ i \frac{b_1}{2M_0} \text{Tr}[\tau^i (k^\mu \mathbf{v}^\nu - k^\nu \mathbf{v}^\mu)] S_\nu , \quad (\text{A.7})$$

Nucleon in, Δ_μ^i and vector source (k_μ) out:

$$- i \frac{b_1}{2M_0} \text{Tr}[\tau^i (k^\mu \mathbf{v}^\nu - k^\nu \mathbf{v}^\mu)] S_\nu , \quad (\text{A.8})$$

Isovector axial source, nucleon, Δ_μ^i :

$$i g_{\pi N \Delta} \text{Tr}[\tau^i \mathbf{a}_\mu] . \quad (\text{A.9})$$

- [1] S.L. Adler and Y. Dothan, Phys. Rev. 151 (166) 1267.
- [2] L. Wolfenstein, in "High-Energy Physics and Nuclear Structure", ed. by S. Devons (Plenum, New York, 1970) p. 661.
- [3] V. Bernard, N. Kaiser and Ulf-G. Meißner, Phys. Rev. D50 (1994) 6899.
- [4] V. Bernard, H.W. Fearing, T.R. Hemmert and Ulf-G. Meißner, Nucl. Phys. A635 (1998) 121.
- [5] H.W. Fearing, R. Lewis, N. Moberg and S. Scherer, Phys. Rev. D56 (1997) 1783.
- [6] G. Bardin et al., Phys. Lett. B104 (1981) 320.
- [7] S. Choi et al., Phys. Rev. Lett. 71 (1993) 3927.
- [8] G. Jonkmans et al., Phys. Rev. Lett. 77 (1996) 4512;
D.H. Wright et al., Phys. Rev. C57 (1998) 373.
- [9] D. Beder and H.W. Fearing, Phys. Rev. D39 (1989) 3493.
- [10] G.I. Opat, Phys. Rev. 134 (1964) B428.
- [11] D. Beder, Nucl. Phys. A258 (1976) 447.
- [12] H.W. Fearing, Phys. Rev. C21 (1980) 1951.
- [13] D. Beder and H.W. Fearing, Phys. Rev. D35 (1987) 2130.
- [14] T. Meissner, F. Myhrer and K. Kubodera, Phys. Lett. B416 (1998) 36.
- [15] S.-I. Ando and D.-P. Min, Phys. Lett. B417 (1998) 177.
- [16] I.-T. Cheon and M.K. Cheoun, nucl-th/9811009.
- [17] H.W. Fearing, nucl-th/9811027.
- [18] T.R. Hemmert, B.R. Holstein and J. Kambor, Phys. Lett. B395, 89 (1997).
- [19] T.R. Hemmert, B.R. Holstein and J. Kambor, J. Phys. G24, 1831 (1998).
- [20] V. Bernard, T.R. Hemmert and Ulf-G. Meißner in "Baryons'98", D.W. Menze and B. Ch. Metsch (eds.) (World Scientific, Singapore, 1999).
- [21] J. Gasser and H. Leutwyler, Ann. Phys. (NY) 158 (1984) 142.
- [22] A.V. Manohar and E. Jenkins, Phys. Lett. B255 (1991) 353; *ibid* B259 (1991) 353.
- [23] V. Bernard, N. Kaiser, J. Kambor and Ulf-G. Meißner, Nucl. Phys. B388 (1992) 315.
- [24] V. Bernard, N. Kaiser and Ulf-G. Meißner, Int. J. Mod. Phys. E4 (1995) 193.
- [25] H. Primakoff, Rev. Mod. Phys. 31 (1959) 802.
- [26] D.V. Balin et al., PSI-proposal R-97-05.1.
- [27] P. Bartsch et al. (A1 Collaboration), MAMI-proposal A1/1-98.

Tables

| Quantity | Symbol | Value | Units |
|-------------------------|----------|-------------------------|-------------------|
| Proton mass | M_p | 938.27321 | MeV |
| Neutron mass | M_n | 939.56563 | MeV |
| Nucleon mass | M_N | 938.91942 | MeV |
| Pion mass | m_π | 139.56995 | MeV |
| Muon mass | m_μ | 105.658389 | MeV |
| Axial-vector coupling | g_A | 1.2670 | – |
| Fine-structure constant | α | 1/137.0359895 | – |
| Fermi constant | G_F | $1.16639 \cdot 10^{-5}$ | GeV^{-2} |
| CKM matrix element | V_{ud} | 0.9740 | – |

TABLE I. Values of the various masses, couplings and other constants used in the text.

| b_1 | $\Gamma_{\text{sing}} [s^{-1}]$ | $\Gamma_{\text{trip}} [s^{-1}]$ | $\Gamma_{\text{tot}} [s^{-1}]$ |
|-------|---------------------------------|---------------------------------|--------------------------------|
| 0. | 0.0031 | 0.1119 | 0.0847 |
| 12. | 0.0029 | 0.1136 | 0.0859 |

TABLE II. Singlet, triplet and total RMC capture rates for the theory with and without delta, respectively. The total rate refers to the para state, i.e. the statistical mixture.

Figures

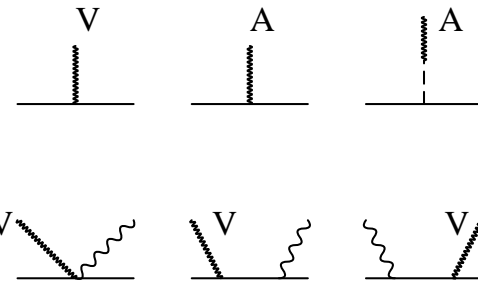


FIG. 1. Graphical representation of the V , A (first row), and VV (second row) correlators. Nucleons, pions, photons and external gauge fields are denoted by solid, dashed, wiggly and zigzag lines, in order.

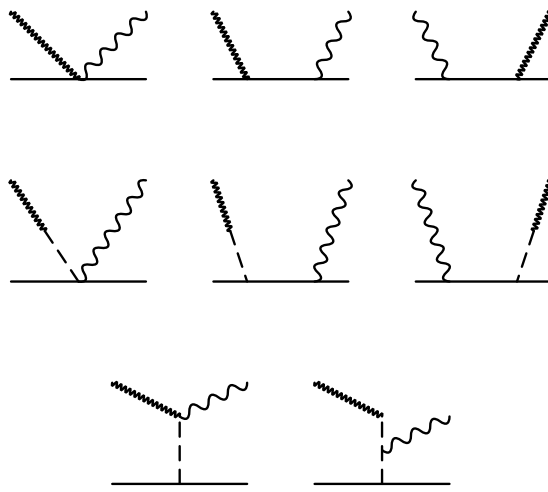


FIG. 2. Nucleon contributions to the VA correlator. All external gauge fields are axial.

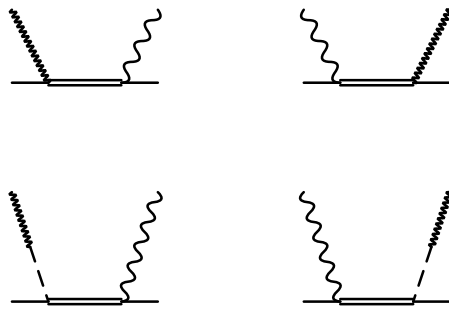


FIG. 3. Delta contributions to the VA correlator. All external gauge fields are axials.

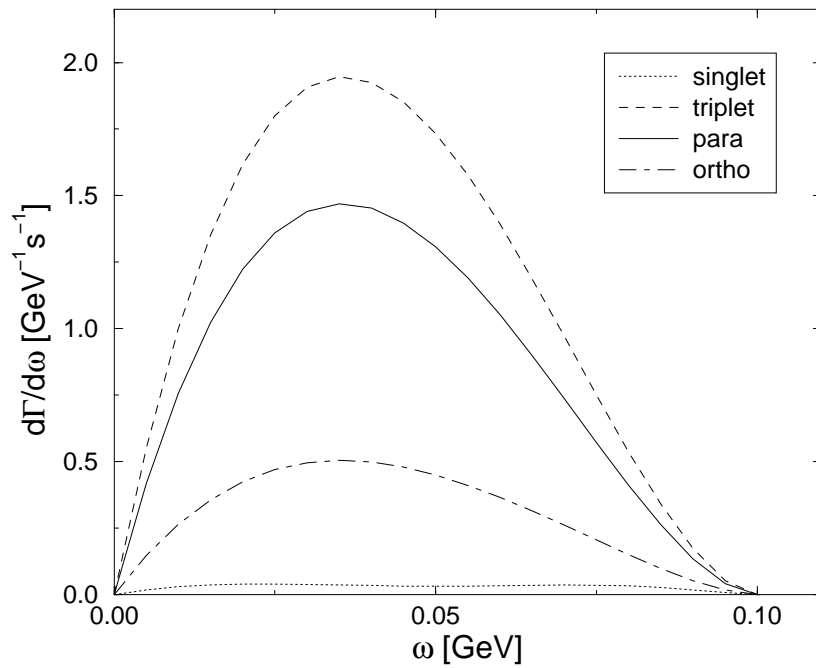


FIG. 4. Photon spectra for RMC for the singlet, triplet, para (statistical) and ortho states of the $\mu - p$ system.

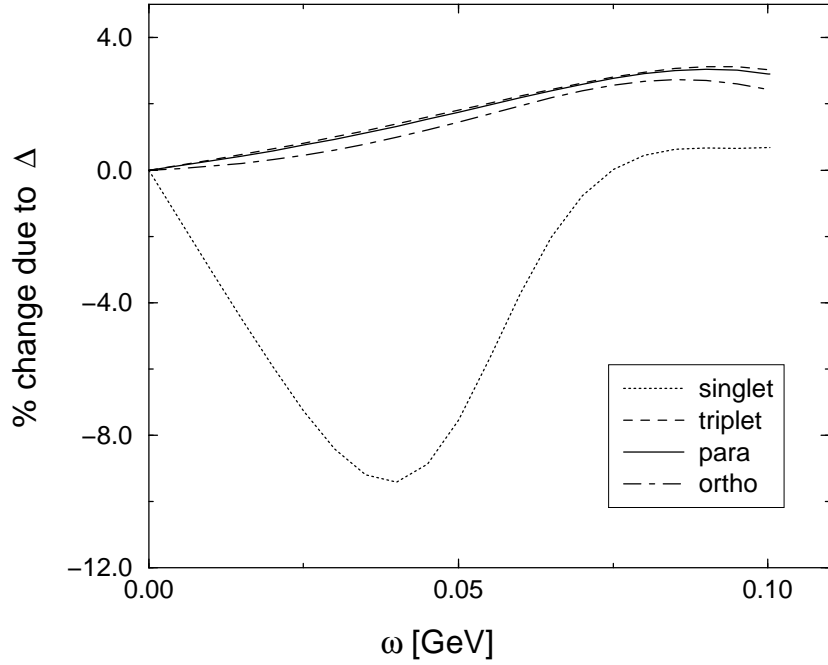


FIG. 5. Relative change in the photon spectra for RMC due to the Δ for the singlet, triplet, para (statistical) and ortho states of the $\mu - p$ system.

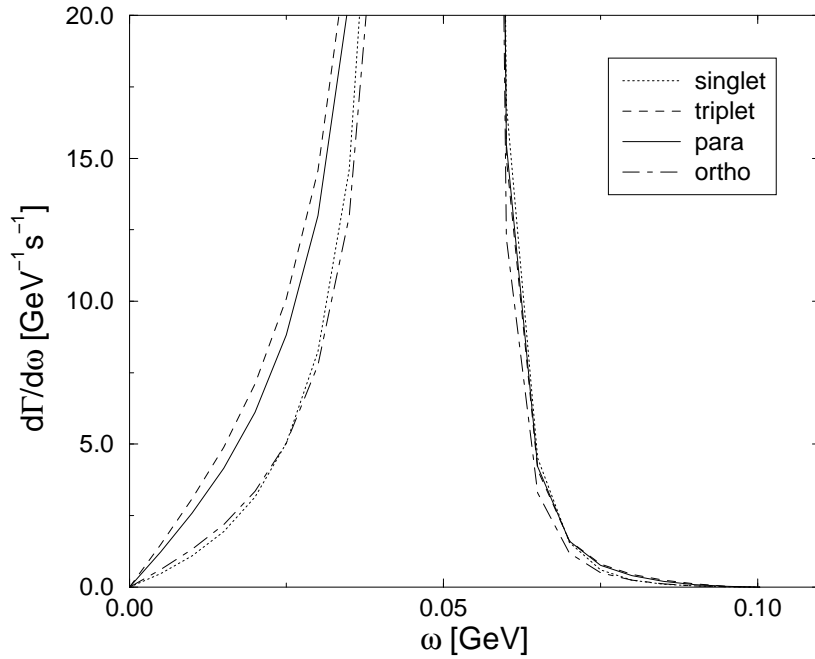


FIG. 6. Photon spectra for RMC for the singlet, triplet, para (statistical) and ortho states of the $\mu - p$ system in the chiral limit (with $b_1 = 0$, i.e. no delta contribution).

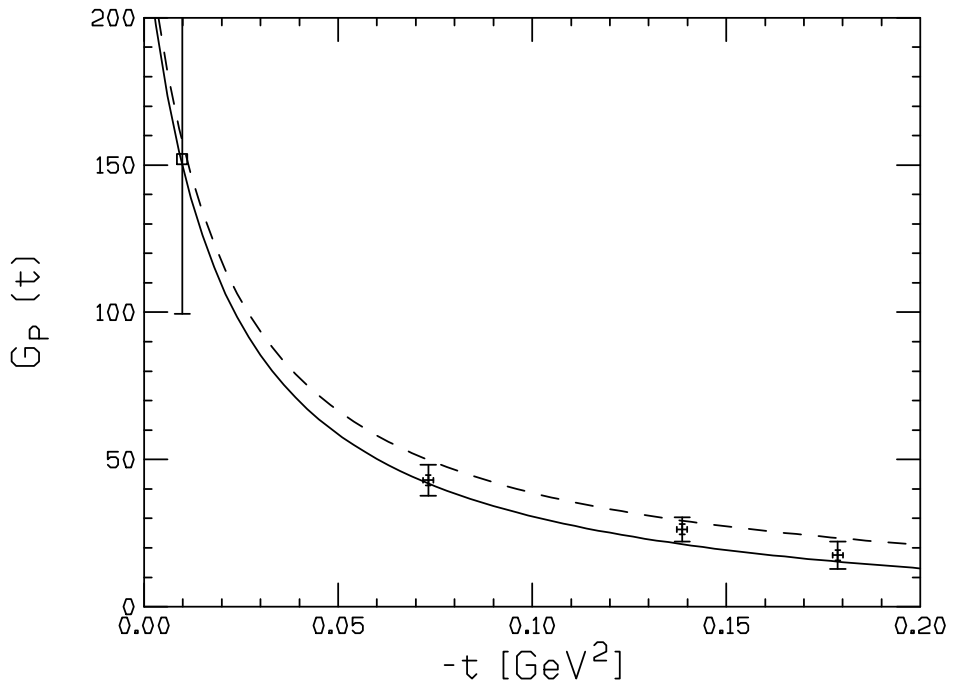


FIG. 7. The “world data” for the induced pseudoscalar form factor $G_P(t)$. Dashed curve: Pion-pole prediction. Solid curve: Full chiral prediction. The pion electroproduction data (crosses) are from ref. [7]. Also shown is the OMC result at $t = -0.88m_\mu^2$ from ref. [6] (open square).

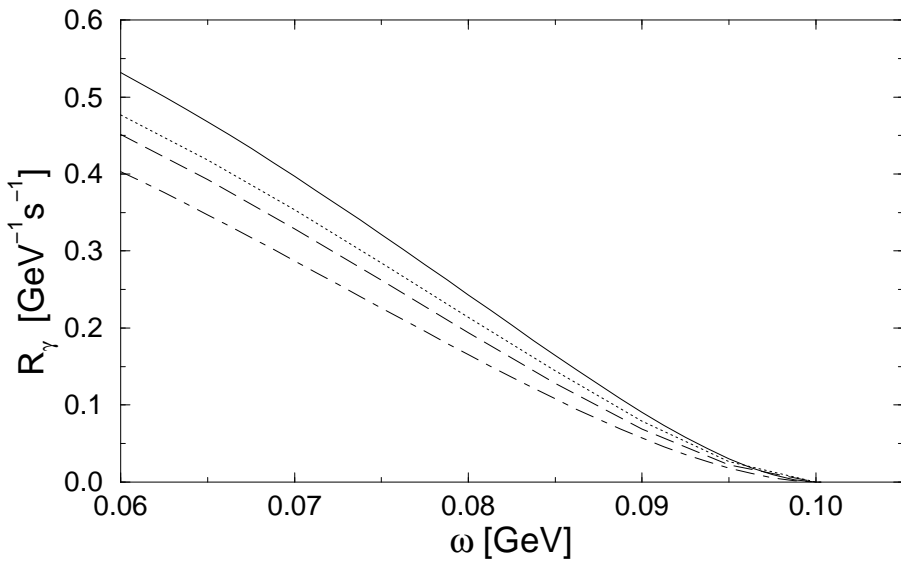


FIG. 8. Photon spectra for RMC for the branching ratios of the singlet, ortho and para states as used in the TRIUMF analysis. Dashed-dotted line: Prediction of the small scale expansion to order ϵ^2 . Solid line: Same as the dashed-dotted line but with g_P scaled by a factor 1.5. Dashed line: Various small modifications as explained in the text. Dotted line: Same as the dashed line but using the neutral instead of the charged pion mass.